

# Crystallization of Poly(L-lactide) in a Confined Space between Polycarbonate Layers

RI-CHAO ZHANG<sup>a\*</sup>, ZHIHUAN HUANG<sup>a</sup>, DAN SUN<sup>b</sup>, AI LU<sup>c</sup>, MEILING ZHONG<sup>a</sup>, ZHENXING FANG<sup>a</sup>, DEHUI JI<sup>a</sup>, GUANGYAO XIONG<sup>a</sup> AND YIZAO WAN<sup>a</sup>

<sup>a</sup>*School of Materials Science and Engineering, East China Jiaotong University, Nanchang 330013, China*

<sup>b</sup>*School of Mechanical and Aerospace Engineering, Queen's University Belfast, UK BT9 5AH*

<sup>c</sup>*Institute of Chemical Materials, China Academy of Engineering Physics, Mianyang, 621900 Sichuan, China*

## ABSTRACT

*In this paper, various thicknesses of PLLA film between PC layers are obtained by spin coating of different amount of solution. The crystal morphologies and isothermal crystallization rates of poly(L-lactide) (PLLA) in the confined spaces between polycarbonate (PC) layers have been studied by polarized optical microscopy. The Crystal morphologies of poly(L-lactide) are little influenced by the thickness of PLLA films between PC layers. Nevertheless, the crystal growth and nucleation rates of PLLA films between PC layers are remarkably affected by the thickness of PLLA films. In the confined space, the nucleation and growth rates of PLLA films decrease as its thickness decreases. The observed phenomena has been ascribed to the reduction of molecular chain mobility, and the slow diffusion process of molecular chains. The results offer greater insights into the materials process-structure-property relationship, and help with design of future biomaterials with tailored/controlled structures/properties (such as crystallinity/ degradation rate) for specific biomedical applications.*

KEYWORD: *Poly(L-lactide), Confined spaces, Polycarbonate, Growth rate, Diffusion*

## INTRODUCTION

Poly(L-lactide) (PLLA), an important biodegradable and biocompatible material, has attracted a lot of interest in biomedical<sup>[1-5]</sup> and

environmental<sup>[6-8]</sup> applications. Particularly, in cell/tissue regeneration applications, the growth kinetics of cells and/or tissues have been remarkably improved on PLLA substrates

---

J. Polym. Mater. Vol. 35, No. 2, 2018, 171-179

© Prints Publications Pvt. Ltd.

Correspondence author e-mail: zrcws@zju.edu.cn, (Ri-Chao Zhang)

designed with appropriate degradation rate<sup>[9,10]</sup>. The degradation of PLLA normally starts from its amorphous phase and subsequently progresses into the crystalline phase from the edges of crystalline lamellar stacks<sup>[11,12]</sup>. As a result, the degradation behavior of PLLA is very much dependent on its crystallinity and crystal structure, which is strongly influenced by the materials crystallization history<sup>[13-18]</sup>. To gain better control of the materials degradation properties and optimize the materials processing parameters, it is important to understand the crystal nucleation and growth process of PLLA.

Crystallization of bulk PLLA has been extensively studied in the past<sup>[13-21]</sup>. Usually, bulk PLLA crystallizes from melt to form spherulites. Double melting behavior takes place when PLLA is crystallized below 120 °C, leading to formation of  $\alpha$  and  $\alpha'$  phases with the same crystal structure but very minor difference in chain conformation and packing density<sup>[19-21]</sup>. Other PLLA crystal morphologies are also possible, e.g., the fibrillar crystal<sup>[22]</sup> can be formed under stress conditions, while dendritic and hexagonal flat-on crystals<sup>[23]</sup> can be formed in thin films with nanoscale thicknesses. Recently, crystallization of PLLA in a confined space both between graphene oxide nanosheets<sup>[24]</sup> and between adjacent spherulites<sup>[25]</sup> has been explored, the resulting PLLA crystalline morphology was suppressed to a two-dimensional mode due to the confined growth spaces. Although several new interesting morphologies have been discovered, especially those achieved in a confined space. In this paper, we aim to carry out a brief study to understand the crystallization process of

PLLA films in a confined space between layers of polycarbonate (PC). The nucleation and growth rates of PLLA with various film thicknesses have been investigated in detail. By adjusting the PLLA film thickness, the nucleation and growth rates of PLLA can be tailored, enabling the fine tuning of the materials crystallinity and crystalline morphology, and potentially, the degradation rates of PLLA products.

## EXPERIMENTAL

### Materials

PLLA with average molecular weight (Mw) of 150,000 g/mol was supplied by Nature Works LLC (USA). Polycarbonate was obtained from Kotex Co. (Japan) and methylene chloride was supplied by Huamei Co. (China).

### Methods

The bulk PLLA film with a thickness of ~0.5 mm was prepared by solution casting method. PLLA-methylene chloride solution (10 w.t.%) was casted into a glass plate and a PC plate, and then kept at room temperature for 24 hours until the solvent is completely evaporated. The obtained PLLA films were further dried in vacuum at 50 °C overnight.

The PC-PLLA-PC sandwiched film structure was fabricated using a KW-4A spin-casting machine (USA) by drop casting a small amount (about 5 ml) of PC methylene chloride solution (10 w.t.%) onto a flat glass substrate and rotate at 6000 rpm for 45 s. The coated substrate is then spin coated with small amount of PLLA, following by another layer of PC using the same procedure after the solvents were totally evaporated, subsequently, to form the sandwich film structure. The thickness of the PLLA film is adjusted according to the concentrations and weight of the PLLA-methylene chloride solution used. The PC-PLLA-PC sandwiched film structure observed under a JEOL 6500F SEM (Japan) with an operating voltage of 5.0 kV is shown in Figure 1. The thickness of PLLA film within the PC-PLLA-PC structure is shown in Table 1.

The morphology of PLLA was observed using a polarized optical microscope (POM) equipped with a CSS450 shear hot stage. The sample was heated to 200 °C and hold for 2 min to allow complete melting, before cooling down to its crystallization temperature ( $T_c$ ) for isothermal crystallization at a rate of 80 °C/min. The radius of the spherulites was recorded as a function of the crystallization time using a calibrated video caliper. The spherulitic growth rates were calculated from the slope of the spherulite radius versus time plots.

TABLE 1. PLLA film in PC-PLLA-PC structure prepared using different amount of PLLA-methylene chloride solutions

PLLA solution content (10 w.t.%)	0.5 ml	1 ml	2 ml	3 ml	5 ml
Thickness of PLLA film ( $\mu\text{m}$ )	2.2	11.3	25.1	52.7	97.9

XRD measurements of PLLA samples after isothermally crystallized at 125 °C for 45 min on glass substrate, PC substrate and between PC films, respectively, were performed under a nitrogen flow using a D8 ADVANCE X-ray diffractometer (Bruker Inc., Germany) with Cu  $K\alpha$  radiation source. The X-ray source was set at a voltage of 40 kV, and the scattering angles  $2\theta$  ranged from 10° to 40°.

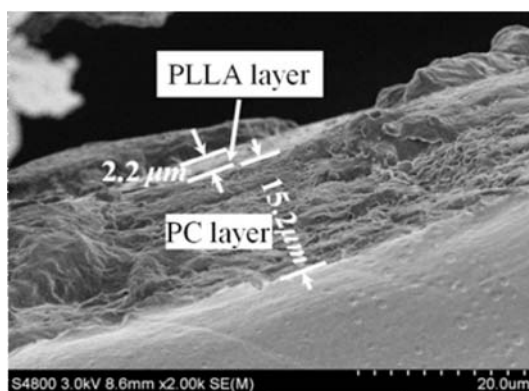


Fig. 1. SEM image of the PC-PLLA-PC sandwiched film structure.

## RESULTS AND DISCUSSION

Previous reports suggest that the morphologies of isothermally melt-crystallized bulk PLLA are mainly spherulitic<sup>[19-21]</sup>. In our present study, perfect spherulites of PLLA isothermally crystallized on the glass substrate at 125 °C have also been observed under the POM, Figure 2, the spherulites shows negative birefringence and the Maltese Cross can be clearly seen. The radius of spherulite increases with the crystallization time until the adjacent spherulites impinge each other.

Fig. 3 represents the POM graphs of PLLA isothermally crystallized on the PC substrate at 125 °C for different times. It appears that the morphology of PLLA is mainly spherulites, which is similar as the results for the sample crystallized on the glass substrate. However, from figure 3 one can find that the number of nuclei for PLLA crystallized on PC substrate is a little more than that crystallized on glass substrate, this is because heterogeneous nucleation takes place when PLLA crystallized on the PC layers, resulting in accelerating the nucleation rate of PLLA when crystallized on the PC substrates.

Figure 4 shows that typically, much fewer spherulite can be observed under POM for the sandwiched PC-PLLA-PC films. Although the morphology of PLLA in the sandwiched PC-PLLA-PC film (thickness of the PLLA film is about 2.2  $\mu\text{m}$ ) is spherulitic, no more nuclei has been observed during the whole crystallization process. This indicates that the thickness of PLLA in PC-PLLA-PC sandwich structure plays a key role in the nucleation of PLLA. Generally speaking, heterogeneous nucleation takes place when PLLA crystallized on the PC layers,

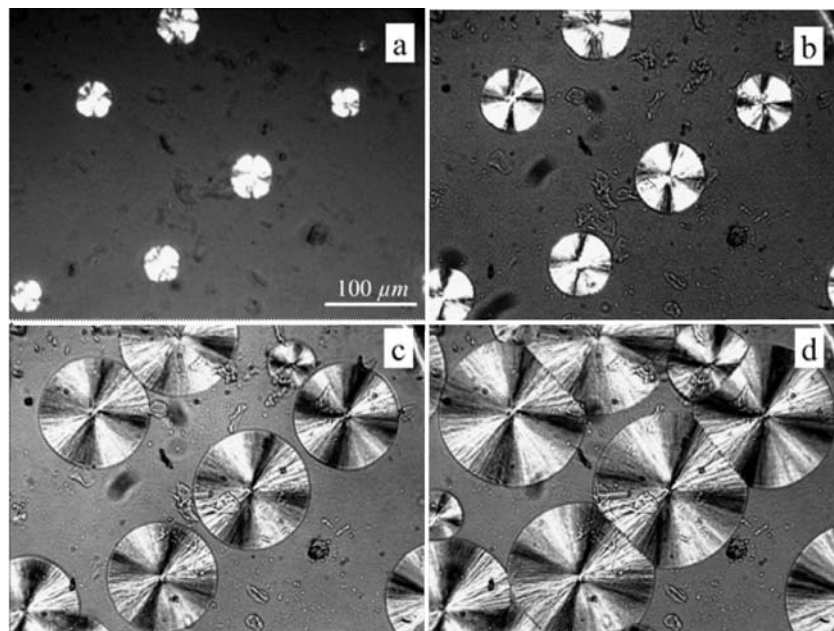


Fig. 2. POM graphs of PLLA isothermally crystallized on the glass substrate at 125 °C for a: 4 min; b: 10 min; c: 20 min; d: 28 min.

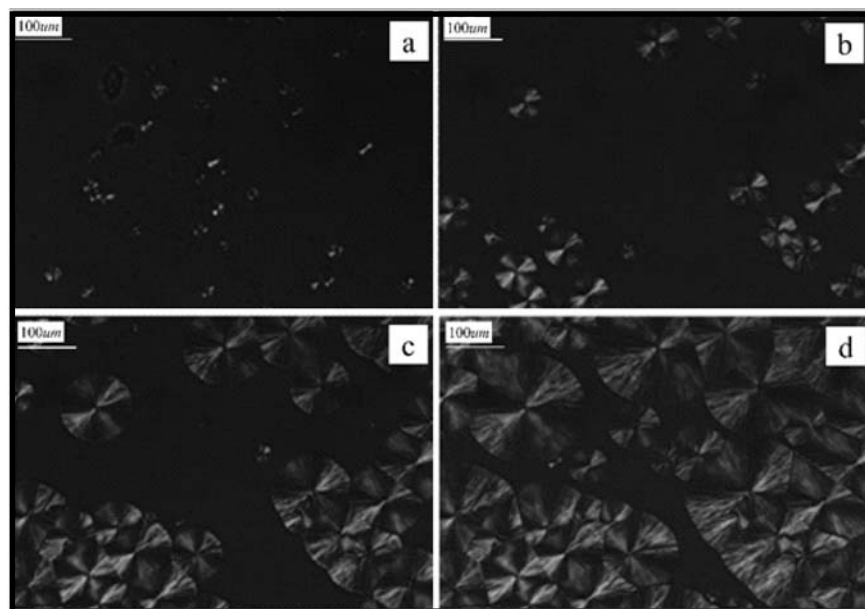


Fig. 3. POM graphs of PLLA isothermally crystallized on the PC substrate at 125 °C for a: 4 min; b: 10 min; c: 21 min; d: 31 min

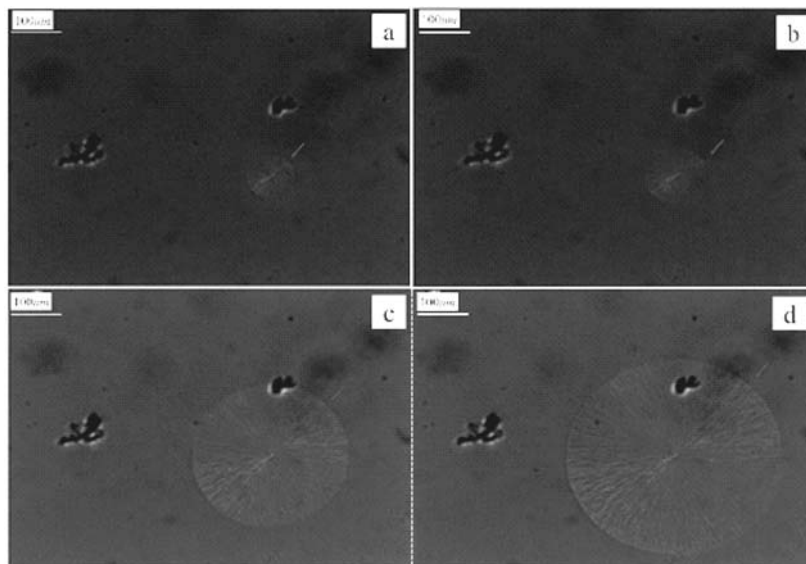


Fig. 4. POM graphs of thin PLLA film ( $2.2 \mu\text{m}$ ) in PC-PLLA-PC sandwich structure isothermally crystallized at  $125 \text{ }^\circ\text{C}$  for a: 6 min; b: 8 min; c: 23 min; d: 30 min.

indicating an accelerated nucleation rate of PLLA should be observed. However, our results show that the nucleation rate of PLLA has been significantly decreased as a result of the reduced PLLA film thickness. According to the previous literature<sup>[26-29]</sup>, the glass transition temperature of a polymer decreases as the thickness of polymer films decreases, resulting in the widening of the  $T_c$  regions. This means the supercooling of the thin PLLA film is decreased compared to the bulk PLLA when crystallized under the same temperature, hence the nucleation rate is slower for the sandwiched PLLA film.

Figure 5a shows the dependence of spherulite diameter on the crystallization time for various PLLA film thicknesses in the PC-PLLA-PC sandwich structure. As expected, the spherulite diameter of PLLA increases linearly with crystallization time. From the plot gradient,

the spherulite growth rate of PLLA with various thickness can be obtained at  $T_c$  of  $125 \text{ }^\circ\text{C}$ , just as shown in Figure 3b. It can be seen from Figure 5b that the spherulite growth rate is greatly affected by the thickness of the PLLA film in the PC-PLLA-PC sandwich structure. The spherulite growth rate increases from  $0.079 \mu\text{m/s}$  for the  $2.2 \mu\text{m}$  film to  $0.091 \mu\text{m/s}$  for the  $97.9 \mu\text{m}$  film. The spherulite growth reaches a plateau ( $\sim 0.091 \mu\text{m/s}$ , similar to that of bulk PLLA) when the thickness of the PLLA film is over  $100 \mu\text{m}$ . The present finding is consistent with past literatures<sup>[30-33]</sup>, where in general, the growth rate of polymers decreases with decreasing polymer film thickness.

Figure 6 shows the spherulite growth rates of the bulk PLLA on glass substrate, PC substrate and the  $2.2 \mu\text{m}$  PLLA film between PC films, respectively, isothermally melt-crystallized at different temperatures. For the bulk PLLA

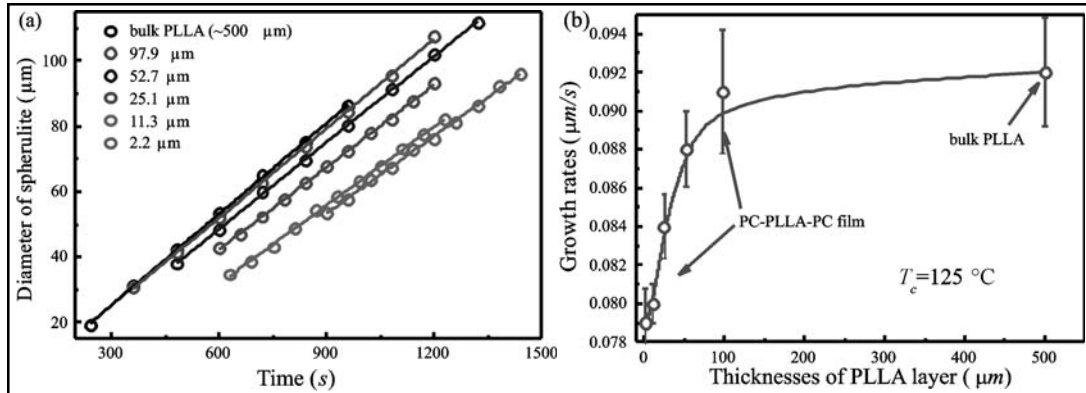


Fig. 5. (a): PLLA spherulite diameter vs. crystallization time; (b): spherulite growth rate vs. thickness for PLLA film isothermally crystallized at  $125^\circ\text{C}$ .

crystallized on glass substrate and PC substrate, the spherulite growth rate peaked at the  $T_c = 125^\circ\text{C}$  and then decreases as the temperature increases further. It is not possible to obtain the spherulite growth rate for  $T_c < 110^\circ\text{C}$ , as the nucleation rate are very fast, resulting in the small spherulites. Moreover, the spherulite

growth rate for these two samples are almost identical when crystallized at the same  $T_c$ . This means that the spherulite growth rate of PLLA has little influenced by the substrate. As for the thin PLLA film (with selected thickness of 2.2  $\mu\text{m}$ ) in the PC-PLLA-PC sandwich structure, the spherulite growth rate increases from 100 to

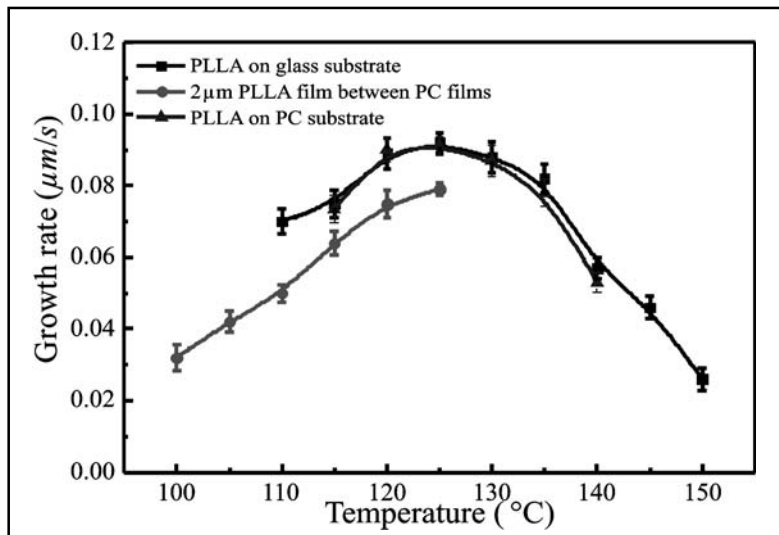


Fig. 6. Dependence of spherulite growth rate on  $T_c$  for PLLA crystallized on glass substrate, PC substrate and between PC films respectively.

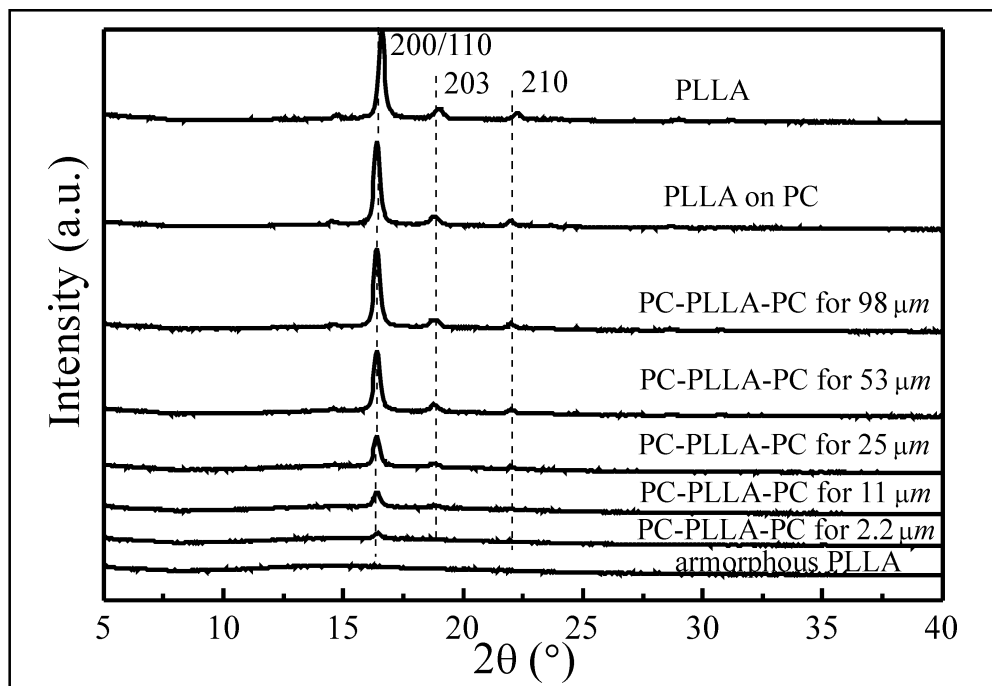


Fig. 7. XRD diffraction patterns of PLLA samples after melt-crystallized at 125 °C for 45 min on glass substrate, PC substrate and between PC films, respectively.

125 °C. Nevertheless, no spherulite has been observed even after 3 hours isothermal crystallization for  $T_c > 125$  °C due to the very slow nucleation rate. It can be seen from Figure 6 that the spherulite growth rate of thin PLLA film is slower than that of the bulk PLLA.

The decreased PLLA nucleation and growth rate with decreasing film thickness can be attributed to the following reasons: 1) the glass transition temperature of PLLA decreases with the thickness of film, resulting in the broadening of the  $T_c$  regions, which decreases the supercooling for the crystallization and slows down the nucleation and growth rate [26-29]. 2) the mobility of the polymer chains is reduced at the PLLA/PC interfaces [30-33]. Considering the molecule chain diffusion near the substrate

is more limited, molecules can be hardly transported to the crystal growth front because of their much lower  $T_g$  comparing to the rest of the film. As a result, the nucleation and growth rate of the PLLA film is further reduced [27-33]. Additionally, the presence of PC on both side of the PLLA film further suppresses the mobility of PLLA molecular chains, creating more barrier towards molecular chain diffusion to the crystal growth front [26-39].

Figure 7 represents the X-ray diffraction patterns of PLLA samples after isothermally crystallized at 125 °C for 45 min on glass substrate, PC substrate and between PC films, respectively. All diffraction patterns have been normalized using the strongest (200)/ (110) reflection intensity. The observed

reflections were indexed on the basis of PLLA  $\alpha$  crystal phase [40–44]. As can be seen from Figure 7, only amorphous peak can be observed for the amorphous PLLA, and the strong reflection peaks (200)/(110) is presented in all crystallized PLLA samples. The intensity of (200)/(110) peak increases as the thickness of PLLA films crystallized between PC films, indicating the crystallinity of PLLA increases. When the thickness of PLLA film is more than 50  $\mu\text{m}$ , the intensity of (200)/(110) peak is almost identical as that of PLLA crystallized on PC and glass substrate. This phenomenon shows that the PLLA film thickness plays a great role in the nucleation and growth rate which finally determines its crystallinity.

### CONCLUSION

In this work, the nucleation and growth rates of the PLLA films in a confined space between polycarbonate has been investigated in details. Results show that the nucleation and growth rates decrease with reduced PLLA film thickness. The presence of PC also contributes to the retardation of the PLLA crystal nucleation and growth by limiting the PLLA molecular chain mobility and their diffusion rate. The results offer greater insights into the materials process-structure-property relationship, and help with design of future biomaterials with tailored/controlled structures/properties (such as crystallinity/degradation rate) for specific biomedical applications.

### ACKNOWLEDGEMENTS

The authors acknowledge financial support from the National Natural Science Foundation of China (contract no. 51203135) and the National

Science Foundation for Young Scientists of Jiangxi Province (Grant No. 20171BAB216020).

### Author Contributions

R.Z. conceived the idea of the work and performed experiments, analyzed the data and wrote the manuscript, D.S., A.L., M.Z, G.X. and Y.W. contributed to data analyses and manuscript writing.

### REFERENCES

1. Y Ikada, Y Shikinami, Y Hara, M Tagawa, E Fukada (1996) *J. Biomed. Mater. Res.* 30:553-558
2. MM Reddy, S Vivekanandhan, M Misra, SK Bhatia, AK Mohanty (2013) *Prog. Polym. Sci.* 38:1653-1689
3. EM Fallahiarezoudar, NM Ahmadipourroudposht, A Yusof, NH Idris, A Ngadiman (2017). *Polymers* 9(11):584
4. HT Wang, PC Chiang, JJ Tzeng, TL Wu, YH Pan, WJ Chang, HM Huang (2017) *Polymers* 9(6):191
5. C Feng, M Piao, D Li (2016) *Polymers* 8(4):165
6. H Li, X Wang, Y Wei, T Liu, J Gu, Z Li, M Wang, D Zhao, A Qiao, Y Liu, (2017) *Polymers* 9(1):20
7. M Forouharshad, L Gardella, D Furfaro, M Galimberti, O Monticelli (2015) *European Polymer Journal* 70:3628-3632
8. P Ma, T Shen, P Xu, W Dong, PJ Lemstra, M Chen (2015) *Acs Sust. Chem. & Eng.* 3:1470–1478
9. EA Makris, P Hadidi, KA Athanasiou (2011) *Biomaterials* 32:7411-7431
10. QL Loh, C Choong (2013) *Tiss. Eng. Part B Rev.* 19:485-502
11. GAR Nobes, RH Marchessault, H Chanzy, BH Briese, D Jendrossek (1996) *Macromolecules* 29:8330-8333
12. PJ Hocking, RH Marchessault, MR Timmins, RW Lenz, RC Fulle (1996) *Macromolecules* 29:2472-2478

13. MC Righetti, M Gazzano, ML Di Lorenzo, R Androsch (2015) *Europ. Polym. J.* 70:215-220
14. ML Di Lorenzo, P Rubino, R Luijckx, M Hérou (2014) *Coll. Polym. Sci.* 292:399-409
15. RC Zhang, D Sun, A Lu, M Zhong, G Xiong, Y Wan (2017) *Polymers* 9(11):625
16. T Shen, P Ma, Q Yu, W Dong, M Chen (2016) *Polymers* 8(12):431
17. P Si, F Luo, F Luo (2016) *Polymers* 8(12):421
18. M Naffakh, C,Marco, G Ellis (2015) *Polymers* 7(11):2175-2189
19. ML Di Lorenzo, P Rubino, B Immirzi, R Luijckx, M Hérou, R Androsch (2015) *Coll. Polym. Sci.* 293:2459-2467
20. A Jalali, MA Huneault, S Elkoun (2016) *J. Mater. Sci.* 51:7768-7779
21. P Pan, B Zhu, W Kai, T Dong, Y Inoue (2008) *Macromolecules* 41:4296-4304
22. P Ma, Q Yu, T Shen, W Dong, M Chen (2017) *Europ. Polym. J.* 87:221-230
23. Y Kikkawa, H Abe, T Iwata, Y Inoue, Y Doi (2001) *Biomacromolecules* 2:940-945
24. Huang HD, Xu JZ, Fan Y, Xu L, Li ZM (2013) *J. Phy. Chem. B* 117:10641-10651
25. S Chen, Y Zhang, H Fang, Y Ding, Z Wang (2013) *Crystengcomm* 15:5464-5475
26. H Schönherr, CW Frank (2003) *Macromolecules* 36:1188-1198
27. H Schönherr, CW Frank (2003) *Macromolecules* 36:1199-1208
28. YX Liu, EQ Chen (2010) *Coord. Chem. Rev.* 254:1011-1037
29. B Lotz, G Li, X Chen, J Puiggali (2017) *Polymer* 115:204-210
30. SN And, M Wübbenhorst (2006) *Macromolecules* 39:5967-5970
31. S Napolitano, M Wübbenhorst (2007) *J. Non-Crys. Sol.* 353:4357-4361
32. Y Zhang, Y Lu, Y Duan, J Zhang, S Yan, D Shen (2004) *J. Polym. Sci. Part B Polym. Phys.* 42:4440-4447
33. Y Zhang, J Zhang, Y Lu, Y Duan, S Yan, D Shen (2004) *Macromolecules* 37:2532-2537
34. S Napolitano, M Wübbenhorst (2007) *J. Phy. Cond. Matt.*, 19:205121.9
35. RM Michell, AJ Müller (2015) *Prog. Polym. Sci.* 54-55:183-213
36. Y Ma, W Hu, G Reiter (2006) *Macromolecules* 39(15):5159-5164
37. G Reiter, JU Sommer (1998) *Physical Review Letters* 80(17):3771-3774
38. D Zhou, J Sun, J Shao, X Bian, S Huang, G Lia, X Chen (2015) *Polymer* 80:123-129
39. G Reiter, G Castelein, JU Sommer, A Röttele, T Thurnalbrecht (2001) *Physical Review Letters* 87(22):b226101
40. D Brizzolara, H.J Cantow, K Diederichs, E Keller, A.J Domb, (1996) *Macromolecules*, 29, 191-197.
41. C. Alemán, B Lotz, J Puiggali (2001) *Macromolecules*, 34, 4795-4801.
42. S Sasaki, T. Asakura, Helix (2003) *Macromolecules*, 36, 8385-8390.
43. Z.Liu, X Liu, G Zheng, K Dai, C.Liu, C. Shen (2015) *Journal of Materials Science*, 50, 599-604.
44. S Liu, F Zhang, G Zheng, K Dai, C.Liu, C. Shen, J.Z Guo. (2016) *Materials Letters*, 172, 149-152.

Received: 10-04-2018

Accepted: 27-06-2018